AGU ADVANCING EARTH AND SPACE SCIENCES

Geophysical Research Letters

RESEARCH LETTER
10.1029/2023GL104949

Antarctic Ice Sheet Freshwater Discharge Drives Substantial Southern Ocean Changes Over the 21st Century

Tessa Gorte[1,2], Nicole S. Lovenduski[1,2], Cara Nissen[1,2], and Jan T. M. Lenaerts[1]

[1]Department of Atmospheric and Oceanic Sciences, University of Colorado Boulder, Boulder, CO, USA, [2]Institute of Arctic and Alpine Research, University of Colorado Boulder, Boulder, CO, USA

Key Points:

- We explore impacts of realistic Antarctic Ice Sheet (AIS) freshwater discharge on the Southern Ocean (SO) using a state-of-the-art climate model
- AIS discharge drives drastic changes in SO stratification, winter deep convection, surface and interior temperature, and sea ice
- Our results suggest that regional AIS discharge can have far-reaching impacts on the SO that can feedback on the climate system

Supporting Information:

Supporting Information may be found in the online version of this article.

Correspondence to:

T. Gorte,
tessa.gorte@colorado.edu

Citation:

Gorte, T., Lovenduski, N. S., Nissen, C., & Lenaerts, J. T. M. (2023). Antarctic Ice Sheet freshwater discharge drives substantial Southern Ocean changes over the 21st century. *Geophysical Research Letters*, *50*, e2023GL104949. https://doi.org/10.1029/2023GL104949

Received 20 JUN 2023
Accepted 20 SEP 2023
Corrected 8 DEC 2023

This article was corrected on 8 DEC 2023. See the end of the full text for details.

Abstract

Multidecadal satellite observations indicate that the Antarctic Ice Sheet (AIS) is losing mass at an accelerating rate, which has the potential to impact many aspects of the climate system. While previous studies demonstrated the importance of AIS freshwater (FW) discharge for regional and global climate processes using climate model experiments, many have applied unrealistic FW forcings. Here, we explore potential Southern Ocean (SO) impacts of realistic AIS mass loss over the 21st century in the Community Earth System Model version 2 by applying observation-based historical and ice sheet model-based future AIS FW forcing. The added FW reduces wintertime deep convective area by 72% while retaining 83% more sea ice. Congruent with other studies, we find the increased FW discharge extensively impacts local and remote SO surface and subsurface temperature and stratification. These results demonstrate the necessity of accounting for AIS mass loss in global climate models for projecting future climate.

Plain Language Summary

We know from several decades of satellite observations that the Antarctic Ice Sheet is losing mass at an accelerating rate. This accelerated mass loss (solid and liquid FW) is often poorly represented—if at all—in global climate models (GCM) and previous studies indicate that even a simple representation of mass loss can have profound climate impacts. Here, we apply a more realistic (in space and time) representation of Antarctic mass loss to a GCM. We find that the added FW leads to more retention of Antarctic sea ice, a decline in wintertime convection of surface waters to the interior ocean, a cooler surface but warmer interior ocean, and a more strongly stratified upper ocean. As such, we argue that properly accounting for Antarctic mass loss in GCMs is imperative for accurately projecting long-term future climate change.

1. Introduction

Since the early 1990s, satellite-based observations have shown that the Antarctic Ice Sheet (AIS) is losing mass. The spatial pattern of AIS mass loss is heterogeneous (Rignot et al., 2019), mostly concentrated in the West Antarctic Ice Sheet (WAIS), which drains into the Amundsen and Bellingshausen Seas in the Southern Ocean (SO) (Velicogna & Wahr, 2006). The Ice sheet Mass Balance Inter-comparison Experiment version 2 (IMBIE2; Shepherd et al. (2018)) estimated that, from 1992 to 2017, the WAIS lost mass at a rate of 94 ± 27 Gt/y, and concluded that this mass loss has been accelerating (Rignot et al., 2019). Several studies using ice sheet models suggest that AIS mass loss will continue to accelerate in the future, as ice shelf thinning, grounding line retreat, and accelerating ice flow are all expected to continue and perhaps intensify with anthropogenic climate change (Gilbert & Kittel, 2021; Noble et al., 2020; Pattyn & Morlighem, 2020).

Apart from rising sea level (DeConto et al., 2021), AIS mass loss will affect many other aspects of the coupled climate system. Observations point to substantial physical changes in SO sea surface height, sea ice, water mass properties, and dense water formation, and a growing body of work attributes these changes to observed increases in AIS freshwater (FW) discharge (hereafter referred to as AIS discharge) (Fasullo & Nerem, 2018; Jacobs & Giulivi, 2010; Li et al., 2023; Purich & England, 2023). The SO's strong teleconnections to the global climate system mean that regional disruptions can precipitate broader changes elsewhere, across a range of timescales (Cabré & Gnanadesikan, 2017). Using climate model projections, previous work suggests that AIS FW fluxes will impact the future evolution of global atmospheric temperature and precipitation (Bronselaer et al., 2018), upper ocean stratification (Aiken & England, 2008; N. C. Swart & Fyfe, 2013), meridional overturning (Moorman et al., 2020; Sadai et al., 2020), and ocean temperature (Bintanja et al., 2015; Park & Latif, 2019; Pauling et al., 2016).

10.1029/2023GL104949

As AIS mass loss is not yet represented interactively in the latest generation of climate models, the potential impacts of AIS discharge on the coupled climate system are often investigated by directly applying anomalous FW fluxes to the ocean component of a climate model. Several studies apply FW forcing around the AIS in a homogeneous fashion (N. C. Swart & Fyfe, 2013; Park & Latif, 2019; Purich & England, 2023)—inconsistent with the observed spatial pattern of AIS mass loss. Others aim to capture future melt of the large Ross and Ronne ice shelves, failing to reflect current grounded AIS mass loss (Bintanja et al., 2013, 2015). Pauling et al. (2016) explore potential impacts of spatially heterogeneous FW forcing but, like others (Aiken & England, 2008; Bintanja et al., 2013, 2015), impose FW abruptly with little to no gradual increase. Both Sadai et al. (2020) and Bronselaer et al. (2018)—which slowly increase the FW flux over several decades—employ global climate models (GCMs) from the Coupled Model Intercomparison Project version 5 (CMIP5) and apply a FW forcing based on CMIP5 Representative Concentration Pathway 8.5 (RCP8.5) runoff projections. These past studies have provided foundational understanding of the sensitivity of the climate system to large-scale AIS mass loss, but are unrealistic in representing the spatio-temporal variability in AIS mass changes and/or do not employ the latest versions of climate models (Landerer & Swenson, 2012).

Here, we apply a spatially heterogeneous FW signal that is reflective of the current spatial pattern of AIS mass loss that increases based on (a) satellite observations for the historical period and (b) CMIP6 Shared Socioeconomic Pathway 5-RCP8.5 (SSP5-8.5) runoff projections for the future period. Furthermore, we leverage the Community Earth System Model version 2 (CESM2), an Earth System Model from the updated suite of models in CMIP6. As we will demonstrate, the modeled SO climate system is highly sensitive to AIS discharge—this discharge drives anomalous trends in vertical density stratification and surface and subsurface temperature as well as the seasonal cycles of sea ice and deep convective area (DCA). Furthermore, our results indicate that regional AIS discharge can impact these processes across the SO basin.

2. Methods

In this paper, we run two fully coupled climate simulations using CESM2. CESM2 is a GCM operated by the National Center for Atmospheric Research, which we ran under historical CMIP6 greenhouse gas forcing from 1970 to 2015 and SSP5-8.5 greenhouse gas forcing from 2016 to 2100 with a $\sim 0.9 \times 1.25°$ horizontal resolution (Danabasoglu et al., 2020). The first simulation, CONTROL, runs from 1970 to 2100 with historical forcing through 2015 and SSP5-8.5 atmospheric forcing from 2016 to 2100. CESM2 preserves mass for the AIS via a mass threshold that, when exceeded, informs the model to transport excess mass to the nearest ocean grid cell as solid ice discharge. For our CONTROL simulation, we override this mechanism, and instead point the model to a prescribed runoff value of 2775 Gt y^{-1} (1 Gt = 1 Gigaton = 10^{12} kg) which is divided into six drainage basins with spatially variable FW discharge that is constant in time (Figure S1 in Supporting Information S1 illustrates the discharge from basal melt and calving assigned to each of the basins derived from Lenaerts et al. (2015)).

The second simulation, IMBIE, branches off of the CONTROL simulation in 1992 and is run out to 2100 under the same forcing conditions. In the IMBIE simulation, AIS FW forcing initially has the same spatial pattern as the CONTROL but is allowed to change in time—we create a more realistic forcing that is observations-based for the historical period (1992–2020) and ice sheet modeling-based for the future period (2021–2100) (DeConto & Pollard, 2016; Rignot et al., 2019). For the observations-based forcing, we apply a linear fit to AIS mass balance data, amalgamated from various products by Rignot et al. (2019) such that FW discharge increases from 2,775 Gt y^{-1} in 1992 to ~3,160 Gt y^{-1} in 2020 with the additional discharge applied solely to the AB Seas basin (Figure S1 in Supporting Information S1). The future AIS FW forcing is based on output from DeConto et al. (2021) who use a combination of ice sheet and climate modeling to estimate the AIS contribution to global mean sea level out to 2300 under RCP8.5 atmospheric warming conditions. Their model output shows steady AIS mass balance through ~2050 after which point, the AIS loses mass non-linearly. To reproduce their findings, our IMBIE FW forcing is constant in time from 2021 to 2050 and increases quasi-exponentially through 2100 ending at a value of 9,098 Gt y^{-1}—slightly higher than the average value for similar exponential experiments (N. C. Swart & Fyfe, 2013) (Figure S1 in Supporting Information S1). Our AIS FW regime corresponds to a total AIS contribution to global mean sea level rise of just over 1 m by 2100. With observations currently indicating that the focus of AIS mass loss is in WAIS, we evenly distribute all of the additional AIS FW flux to the surface coastal grid cells in the co-located drainage basin in the Amundsen and Bellingshausen Seas (AB Seas; 95°W to 145°W) (Figure S1 in Supporting Information S1). We also subdivide our FW forcing into its solid (calving) and liquid (basal melt) components. Each basin has its own ratio of solid to liquid FW based on results from Depoorter et al. (2013) and these ratios are held constant for the entirety of the simulations (Figure S1 in Supporting Information S1). Over the AIS, calving and basal melt account for ∼48% and ∼52%, respectively.

For this paper, the SO is defined as the ocean south of 50°S and we explore upper ocean stratification, DCA, surface and interior ocean temperature, and sea ice extent (SIE) over this region by averaging across all points south of 50°S. We quantify upper ocean stratification as the difference of the potential density at 200 m and that at the surface ($\Delta\rho_{200-\mathrm{surf}} = \rho_{200} - \rho_{\mathrm{surf}}$) such that positive numbers correspond to higher densities at depth (i.e., stable stratification). DCA is calculated as the combined grid cell area under which the maximum mixed layer depth exceeds 50% of the bathymetry (Heuzé, 2021; Heuzé et al., 2013). As such, DCA is purely a metric for how well the water column is mixed. Its existence can be—but is not necessarily—related to the formation of precursors of Antarctic Bottom Water which ultimately depends on the density of the waters involved. CESM2 is one of the few CMIP6 models that produces deep convection solely in the coastal regions with no dense shelf water (DSW) formation in the open ocean (Heuzé, 2021) due to its pipe-like overflow parameterization that transports DSW to deeper basins (Danabasoglu et al., 2020). We define the surface ocean as the topmost vertical layer of the ocean model in CESM2 (10 m thick) and consider anything below the mixed layer (∼100–150 m) to be the interior ocean. Because we only have one ensemble member each for CONTROL and IMBIE, we are unable to fully evaluate the changes within the context of internal variability. To provide more robust statistics for our analysis, we take multidecadal (20-year) means from the beginning of the simulation (1992–2012) and end of the simulation (2080–2100).

3. Results

Meltwater changes the density structure of the SO, resulting in enhanced upper ocean stratification (Figure 1). The SO-averaged difference in stratification, $\Delta\rho_{200-\mathrm{surf}}$, increases for both simulations but significantly more so in the IMBIE simulation (1A). For the entire 1992–2100 simulation period, the IMBIE simulation $\Delta\rho_{200-\mathrm{surf}}$ increases by approximately 0.2 kg m^{-3} (44%) while the CONTROL simulation, by comparison, increases by 0.05 kg m^{-3} (16%). The difference in SO stratification between the two simulations is largely realized in the latter half of the 21st century with much of the increase in the IMBIE simulation occurring after 2070. The spatial realization of the enhanced stratification is such that the signal in the IMBIE is largely focused in the AB Seas region but also present in the Ross and Weddell Seas (Figures 1b and 1c). In these areas, the increase in stratification can be upwards of 1 kg m^{-3} which constitutes a first order of magnitude change on the historical mean state (Figure S3 in Supporting Information S1). Whereas, the CONTROL simulation shows no significant change in stratification over the course of the 21st century in these regions. Rather, the CONTROL simulation indicates a small increase in stratification in the open SO, that is also captured in the IMBIE simulation (Figures 1b and 1c).

AIS discharge is associated with a significant reduction in SO DCA (Figure 2). CESM2 develops deep convection in many Antarctic coastal regions in the historical simulation (Figure 2, yellow regions on map insets). Over the course of the century, both the CONTROL and IMBIE simulations project a decline in SO DCA from June through December, when DCA is at a maximum (Figure 2a). Austral winter DCA declines by 17% in the CONTROL simulation over the century, driven by anthropogenic changes other than AIS discharge (e.g., warming). Whereas, in the austral summer when the DCA is at a minimum, there is no statistically significant change in DCA over time or between simulations (Figure 2a). Including the effects of AIS discharge leads to a wintertime DCA reduction from a median value of 0.34–0.24 Mkm^2; ∼29% (Figure 2a). Even with the 29% reduction in wintertime SO DCA in the IMBIE simulation, the median DCA for every month is within the extrema for the CONTROL (Figure 2a). This reduction in maximum DCA manifests as the initiation production of less dense surface water (below 35.5 kg m^{-3}) as well as significantly less DSW formation. By the end of the century, the CONTROL simulation produces 54% more DSW than the IMBIE simulation—increasing from 33% from 1992 to 2007—solely as a result of buoyancy-driven changes (Figure S2 in Supporting Information S1).

The AIS discharge-related reduction in SO DCA manifests most strongly in the AB Seas, where our model simulation projects a 75% decline in DCA in the austral winter months in the IMBIE simulation. Compared to a 13% decline in DCA for the CONTROL, this indicates substantially reduced seasonal DCA variability (Figure 2b). By the end of the century, the medians for the months of May as well as August through November are outside the extremes of the CONTROL DCA. The median CONTROL DCA in this region is also reduced from August–November but is within the historical DCA distribution. The Ross Sea, whose DCA historically varies between

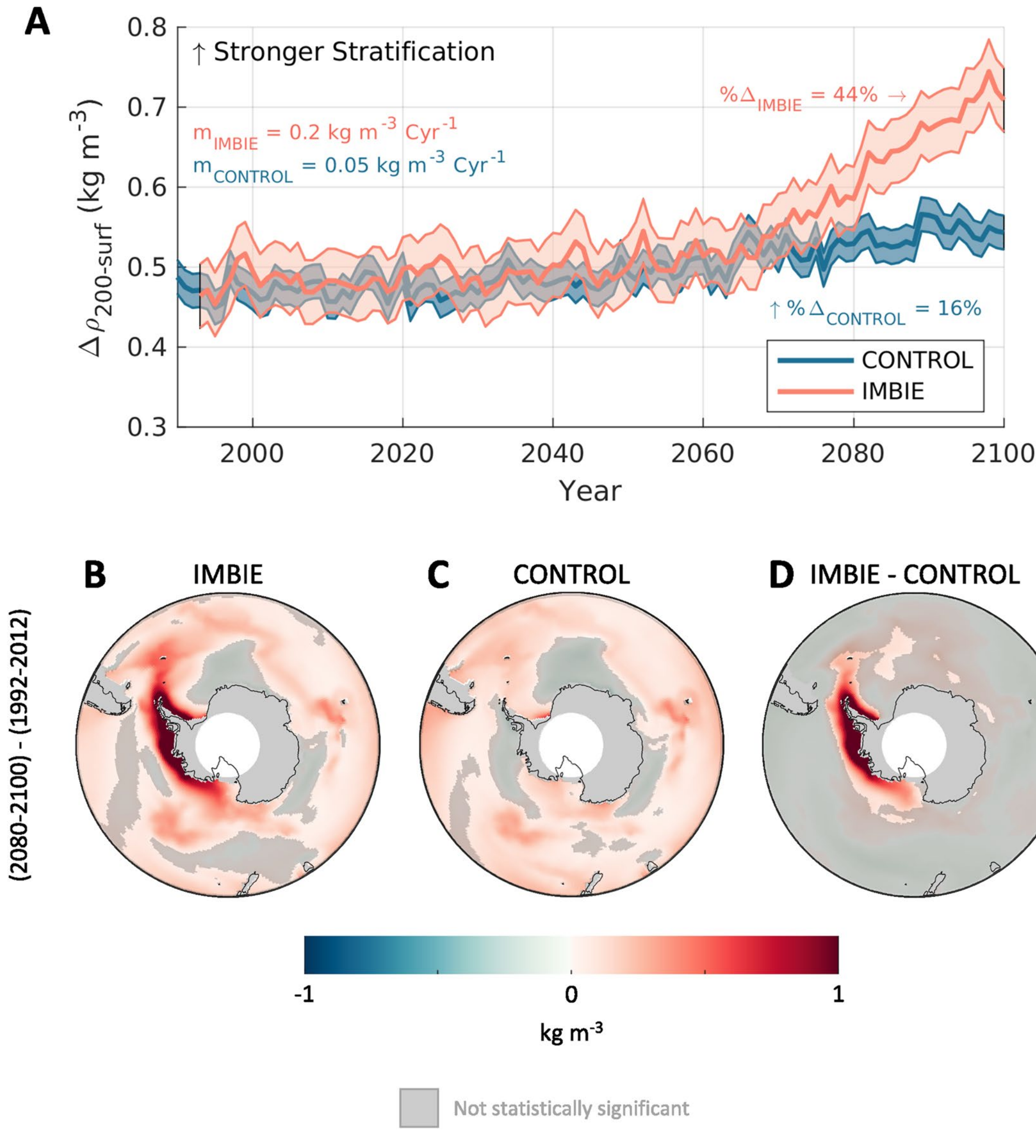

Figure 1. (a) Temporal evolution of the Southern Ocean (SO) potential density difference spatially averaged south of 50°S, between the surface and 200 m depth ($\Delta\rho_{200-\mathrm{surf}}$) over 1990–2100 for both the CONTROL (blue) and IMBIE (peach) simulations. Larger numbers indicate stronger stratification. The solid line shows the SO average for each simulation and the shading indicates 1-σ where σ is the detrended annual mean time series of $\Delta\rho_{200-\mathrm{surf}}$ in each simulation. Panels (b)–(c) end-of-century (2080–2100) minus beginning-of-century (1992–2012) $\Delta\rho_{200-\mathrm{surf}}$ in the IMBIE and CONTROL simulations, respectively. (d) Map of panel (b)—panel (c) showing the difference in the temporal evolution of stratification between the two simulations. Darker reds indicate stronger stratification with non-statistically significant changes shaded in gray. Statistical significance, here, indicates grid cells where the change from the beginning to the end of the century exceeds the interannual variability of the historical period in the CONTROL simulation.

~0.04–0.1 Mkm^2 in the austral winter and spring shows a 52% reduction in DCA in the IMBIE simulation and a 30% reduction in the CONTROL from July–November. The median IMBIE DCA is within the broad (and thus highly variable) historical distribution of DCA for the Ross Sea. As such, our simulations indicate that AIS discharge reduces deep convection both regionally in the AB Seas as well as in regions outside of where the FW forcing is applied, such as the Ross Sea.

AIS discharge leads to anomalous cooling in the surface and anomalous warming in the subsurface of the SO. The surface and subsurface SO warm ubiquitously in both simulations with anthropogenic climate change (Figures S4–S7 in Supporting Information S1). The surface SO warms 0.28°C less in the IMBIE simulation than in the CONTROL by 2100 (1.8 and 1.5°C respectively). This anomalous cooling, which extends through the mixed

10.1029/2023GL104949

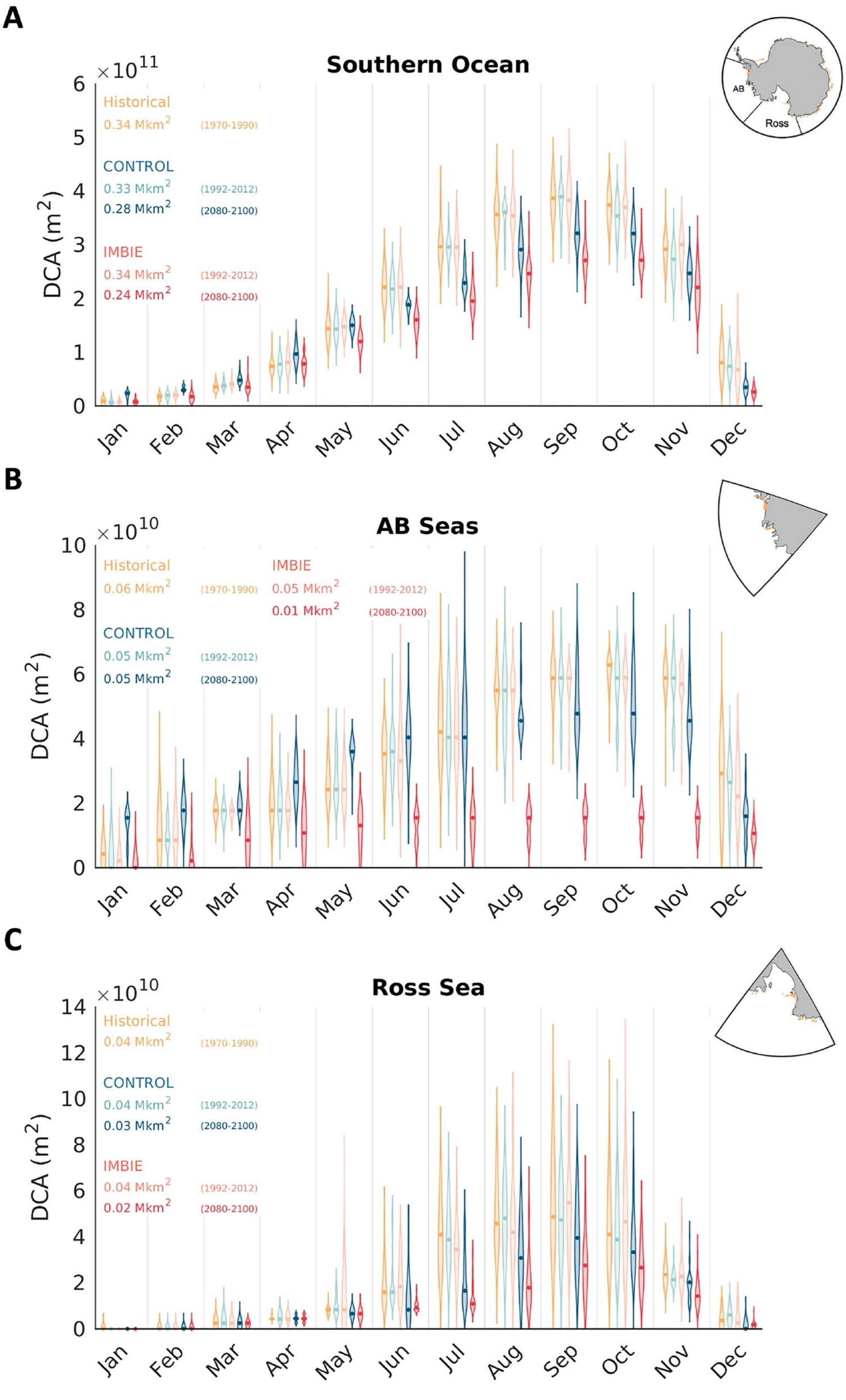

Figure 2.

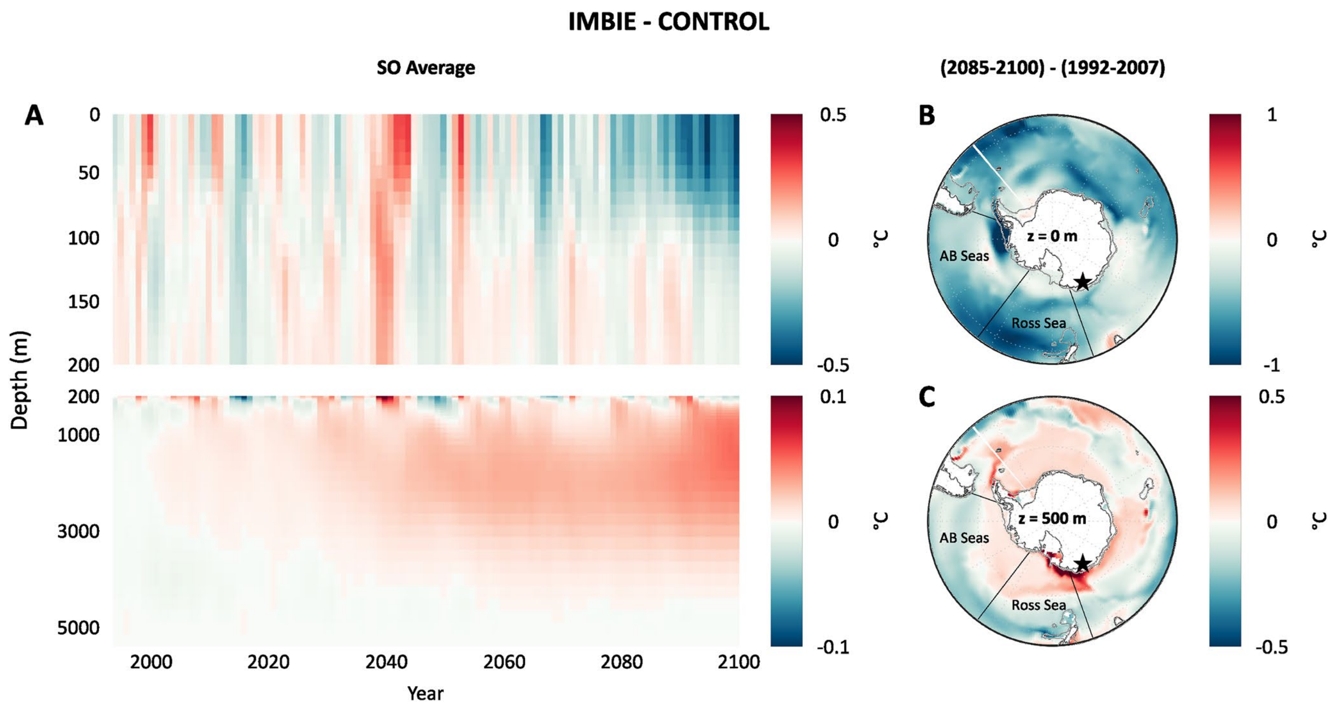

Figure 3. (a) The difference in average Southern Ocean (SO) vertical temperature profile averaged over all points south of 50°S, from 1992 to 2100 between the IMBIE and CONTROL simulations from 1992 to 2100. The upper panel depicts the top 200 m of the SO and has values ranging from −0.5 to 0.5°C; the lower panel depicts 200 m to the ocean floor with values ranging from −0.1 to 0.1°C. Bluer (redder) colors indicate when and at what depth the IMBIE simulation is cooler (warmer) than the CONTROL. (b) Difference (IMBIE-CONTROL) in SO surface temperature evolution comparing the 2080–2100 period to the 1992–2012 period. (c) Map of the difference (IMBIE-CONTROL) in SO 500 m depth temperature evolution comparing the 2080–2100 period to the 1992–2012 period. Black lines denote the boundaries of the AB Seas and Ross Sea regions. A black star denotes coastal Adélie Land in panels (b) and (c).

layer (∼100 m), begins to appear mid-century, and intensifies after ∼2070 (Figure 3a). Anomalous surface ocean cooling in response to AIS discharge manifests most strongly in the AB Seas region, where we impose the strongest FW forcing (Figure 3b). Here, surface temperatures from the IMBIE simulation are nearly 2°C cooler than those in the CONTROL simulation. Another area of anomalous cooling due to FW input manifests off the coast of the East AIS near Enderby Land; a region of low SIE.

In contrast to the surface cooling, the deep SO (500–3,000 m) experiences anomalous warming with AIS discharge over the course of the century. Averaged over the SO, the IMBIE simulation warms by 0.70°C compared to 0.63°C in the CONTROL. As such, the IMBIE simulation is 0.07°C warmer than the CONTROL on average between 500 and 3,000 m depth by the end of the century (Figure 3a). The anomalous warming of the deep SO is spatially heterogeneous. Figure 3c shows anomalously warm temperatures (∼0.1°C) extending from the coast northward to the core of the Antarctic Circumpolar Current, with much larger anomalies (0.89°C) in the Ross Sea and along the Adélie Coast at 500 m. Notably, this pocket of anomalously warm water is not co-located with the AIS FW input.

Both simulations show an overall loss of sea ice over the 21st century with anthropogenic climate change, however, the IMBIE simulation shows significantly less extensive sea ice loss, especially in the austral winter/spring (July–November). The historical SO sea ice cover is largely circumpolar with the highest concentrations in the Weddell and Ross Seas (Figure 4a). By the end of the century (2080–2100) the IMBIE simulation retains over 50% more sea ice in the AB Seas region (Figure 4b). The Weddell and Ross Seas—particularly out at the sea ice edge near the peninsula—also preserve over 25% more sea ice than the CONTROL (Figure 4b). Historical SIE

Figure 2. Monthly deep convective area (DCA) climatology from the (yellow) 1970–1990 historical, (light blue) 1992–2012 CONTROL, (dark blue) 2080–2100 CONTROL, (peach) 1992–2012 IMBIE, and (red) 2080–2100 IMBIE periods/simulations averaged over the (a) Southern Ocean, (b) Amundsen/Bellingshausen Seas, and (c) Ross Sea regions. Maps in the upper right of each panel depict the region of interest as well as the historical DCA (yellow). The violin plots for each month represent the kernel density of DCA distribution. Each violin plot has a dot denoting the median DCA and the ends of the plot extend out to the extrema of the distribution.

10.1029/2023GL104949

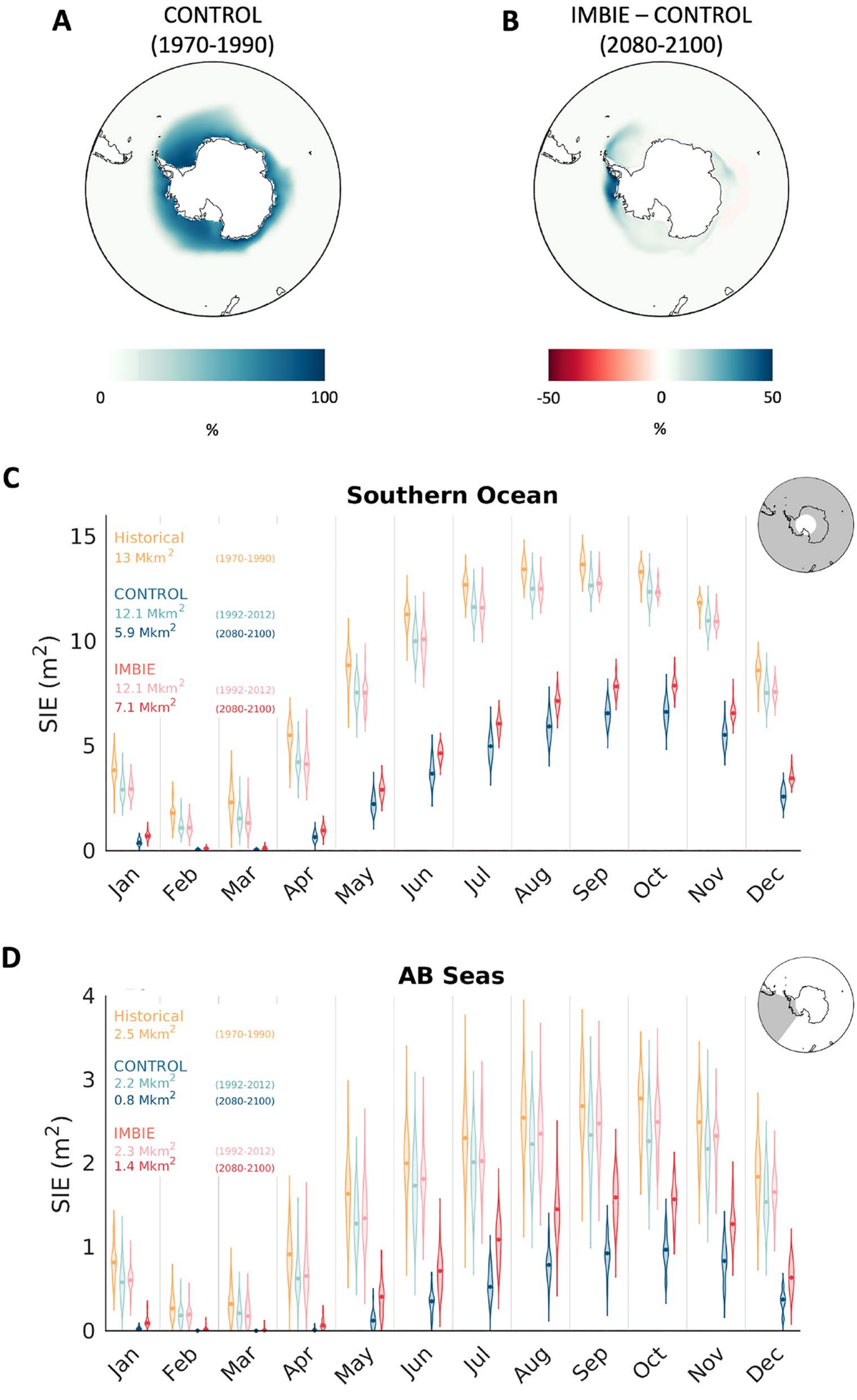

Figure 4. (a) Average annual mean of sea ice fraction in each grid cell for the 1970–1990 historical period. (b) the average difference in sea ice fraction between the IMBIE and CONTROL simulations during the 2080–2100 period. (c) Monthly sea ice extent (SIE) for the whole Southern Ocean in the historical (yellow), 1992–2012 CONTROL (light blue), 2080–2100 CONTROL (dark blue), 1992–2012 IMBIE (peach), and 2080–2100 IMBIE (red) periods. The violin plots for each month represent the kernel density of SIE distribution. Each violin plot has a dot denoting the median SIE and the ends of the plot extend out to the extrema of the distribution.

typically reaches an annual maximum in September-October and an annual minimum between February-March and can vary between 2 and 15 Mkm^2, seasonally, across the entire SO (Figure 4d). In the AB Seas, SIE varies between 0.25 and 3.25 Mkm^2. For both the AB Seas as well as the entire SO, there is a significant decline in SIE from the 1992–2012 period to the 2080–2100 period, driven by anthropogenic climate change (Figures 4c and 4d). However, there is a significant difference in SIE between the IMBIE and CONTROL simulations by the end of the century, particularly in the austral winter and spring (Figures 4c and 4d). For 5 months out of the year, the IMBIE simulation produces over 1 Mkm^2 more total SO sea ice than the CONTROL in the 2080–2100 period with the maximum, 1.3 Mkm^2 in September, equivalent to ~9% of the total historical SIE (Figure 4c). This disparity in SIE is largely due to more sea ice preservation in the AB Seas region, which retains nearly 20% more sea ice in the IMBIE simulation compared to the CONTROL (Figure 4d).

4. Conclusions and Discussion

To investigate the potential role of projected AIS discharge on the SO, we conducted analysis using two fully coupled climate simulations with identical atmospheric forcing but different AIS FW fluxes. AIS discharge anomalously increases upper ocean stratification by ~30% across the SO, with large increases in the AB Seas, and smaller increases in the Weddell and Ross Seas. End-of century SO wintertime DCA is 0.34 Mkm^2 in the control simulation, but only 0.24 Mkm^2 in the IMBIE simulation. Regionally, we see the strongest impacts in the AB Seas region as wintertime DCA is reduced to summertime levels while DCA in the Ross Sea declines by ~22% due to the FW. Both simulations show an increase in DSW; IMBIE by 3.5% and the CONTROL by 16%. In addition to the diverging DSW trends over time, the added FW initiates the formation of lighter DSW the latter of which is consistent with results from Nissen et al. (2022) who show that buoyancy-driven changes in the Weddell Sea reduce the potential for DSW to be transported to the deeper open ocean. The IMBIE surface ocean is 0.28°C cooler than that of the CONTROL while the subsurface warms significantly with warmer regions focused in the western Ross Sea and along the Adélie Land coast. Our simulations also project that the freshening and anomalous cooling of the surface SO induce conditions more favorable for sea ice formation.

Our results suggest that the freshening of the AB seas, and to a lesser extent, the broader SO, is the primary driver of the enhanced stratification in the IMBIE simulation. Surface temperature cools while subsurface temperature warms in response to AIS discharge, a change that would induce reduced stratification if no salinity anomalies were present. The freshening and anomalous cooling of the surface SO induce conditions more favorable for sea ice formation. Previous studies have noted the importance of the ice-albedo feedback wherein when sea ice melts, it exposes the darker surface ocean below, lowering the albedo, increasing ocean heat uptake, inducing more sea ice melt and/or less sea ice growth (Curry et al., 1995). With the IMBIE simulation preserving more sea ice than the CONTROL, this positive feedback loop is suppressed, and the surface ocean is relatively cooler. When sea ice forms, however, it releases heat and rejects highly saline brine, decreasing sea surface temperature while increasing sea surface salinity. The lower surface temperature and salinity in the IMBIE simulation, then, implies that the heat uptake (or lack thereof) and the FW discharge dominate the sea ice formation signal for the evolution of both variables. The FW in the surface ocean overwhelms any enhanced convection induced by brine rejection from the relatively larger SIE in the IMBIE simulation. FW-induced changes to stratification and DCA as well as surface and interior temperature all permeate into more remote regions of the SO, mainly the Ross and Weddell Seas. Deep convection, which only occurs in coastal grid cells, is most strongly affected in the AB Seas but also manifests remotely in the Ross Sea. The loss in DCA is realized predominantly from July–November such that the historical wintertime high is reduced to summertime low levels in the AB Seas. Historically, the AB Seas region is not considered a major contributor to DSW formation so these results do not drive prominent changes to total SO DSW formation or deep convection. The DCA loss aligns temporally with the highest sea ice retention—most of the preserved sea ice exists in the AB Seas and, to a lesser extent, the Ross and Weddell Seas. As these processes evolve and feedback into one another, they become fundamentally convoluted. To extricate the impacts of any given variable on the evolution of another requires further sensitivity testing.

Our findings are supported by those reported in other studies. Compared to Bronselaer et al. (2018), Sadai et al. (2020), and Purich and England (2023), our SIE and surface and interior temperature manifest similarly in strength and spatial pattern with much of the AB Seas sea ice persisting despite strong anthropogenic warming and anomalous warming of the western Ross Sea. Similar surface cooling from enhanced FW fluxes also appear in Greenland Ice Sheet FW experiments (Menviel et al., 2015). We find the sea ice response to be significantly less than what was found in the ice-shelf specific sensitivity experiments of Bintanja et al. (2013, 2015). While we do see a differential sea ice response by the end of the century, the FW-induced changes are not statistically significantly different until after 2070; nearly 80 years into the simulation. As such, we find the minimal sea ice response in extent and trend over <50 model years as seen by N. C. Swart and Fyfe (2013) and Pauling et al. (2016), respectively, to be consistent with our results. Bintanja et al. (2013) find that the strength of their FW forcing engenders a sea ice response strong enough to account for the disparate observed SO sea ice cover. Our historical SO sea ice cover, which peaks at ∼15 Mkm^2 in September, is already lower than the observed 18–20 Mkm^2 in September SIE. Likely owing to anthropogenic warming, there is a significant overall reduction in SO SIE on the order of ∼5–8 Mkm^2 with the IMBIE simulation retaining ∼1 Mkm^2 more than the CONTROL by the end of the century. That is to say, the FW discharge does help preserve SO SIE but not enough to offset anthropogenic warming. Like Park and Latif (2019) and Li et al. (2023), we also see a decline in deep convection in the SO. Park and Latif (2019), use a model noted for producing too much open ocean deep convection Heuzé (2021) while Li et al. (2023) use a high-resolution ocean-sea ice coupled model with reasonable DSW formation. Heuzé (2021) notes CESM2's lack of open-ocean deep convection which is consistent with our results. Difficulties that arise from the overflow parameterization—the process by which CESM2 transfers DSW to deeper basins—impedes quantifiable assessments of offshore transport.

There are three major caveats with this work: (a) the assumption that past observations are a good predictor of future changes, (b) the assumption of ice shelf mass (im) balance, and (c) the application of our FW forcing. We assume that past AIS melt patterns will continue into the future. Our understanding of the decades-to-centuries long spatio-temporal changes to AIS mass balance is limited, as mass change records from the GRACE satellite missions are only 20 years long. Ice sheet models—which are informed by these and other observations—project sustained elevated mass loss in the West AIS region over the course of the next century (DeConto & Pollard, 2016). Further, the GRACE satellites only measure the mass balance of the grounded ice sheet, not the ice shelves, leaving us with little information about large-scale ice shelf mass (im) balances across the AIS. In addition, CESM2 cannot model floating ice shelves. As such, we assume that the AIS ice shelves are in mass balance and that continental mass changes are directly realized as FW fluxes. These FW fluxes, then, are introduced solely to the coastal surface grid cells, though previous work indicates that similar GCMs are sensitive to neither the horizontal FW distribution close to or far from the coast nor the vertical FW distribution—FW fluxes applied at the surface compared to the interior ocean deepens the mixed layer but has little overall impact on sea ice formation and vertical advection in the SO over ∼3 decades—meaning our FW flux spatial distribution is reasonable for this assessment Bronselaer et al. (2018) and Pauling et al. (2016). Finally, we leverage observed AIS mass changes from the GRACE satellites to guide historical (1992–2020) FW discharge and GCM output for future (2021–2100) discharge. The GCM (CESM1) projection we use for future AIS mass balance is (a) based on a model that doesn't have an active ice sheet and, thus, inherently misses any feedbacks with the coupled climate system and (b) generally constant until about 2050, after which point, it increases dramatically (DeConto et al., 2021). Stitching these two forcings together, then, means that from 2021 to 2050, there is a constant annual FW forcing from the AIS that is guided by limited information.

Another caveat of this work is the choice of atmospheric forcing scenario under which we ran our simulations. The projected FW forcing is based on climate model output which employed the RCP8.5 atmospheric forcing (DeConto et al., 2021). Recent work has indicated that this scenario best tracks current estimates of CO_2 emissions (Schwalm et al., 2020). That said, Trusel et al. (2015) show that AIS surface meltwater production can vary by a factor of 2.5× just between RCP8.5 and RCP4.5 by 2100. As such, the choice of forcing scenario will likely have a large impact on the magnitude of FW fluxing of the AIS. Additionally, previous work has found that coarse-resolution models (1 × 1) produce large-scale open-ocean freshening, severely limiting polynya events which are critical for generating deep convection on the shelves citing enhanced AIS runoff as a contributing factor to the FW signal (Lockwood et al., 2021). The reduction of SO polynyas and subsequent decline in DSW mean that AIS FW fluxes act partially as a parameterization of DCA and DSW. Furthermore, finer resolution models allow for the homogenization of shelf water masses, engendering changes in a more circumpolar manner (Moorman et al., 2020). Thus, the resolution of our simulations (1 × 1) could be a large factor in driving the heterogeneity of our results. Given CESM2's resolution, the Antarctic Slope Current is not fully resolved which impacts the simulated shelf properties and the processes by which FW perturbations are transported to the open ocean (Lockwood et al., 2021).

Our results nevertheless demonstrate the potential ramifications of AIS FW discharge on the climate system. AIS FW is likely to play a key role in the spatio-temporal evolution of the SO over the 21st century. Given the importance of the SO for the uptake of anthropogenic heat and carbon (Frölicher et al., 2015), it is reasonable to expect that AIS FW discharge will engender climate feedbacks in the coming century and beyond.

Data Availability Statement

Data from the CONTROL simulation presented in this paper are publicly available at Gorte et al. (2023a). Data from the IMBIE simulation presented in this paper are publicly Gorte et al. (2023b).

Acknowledgments
We would like to thank Dr. Leo van Kampenhout for his work in the setup of these experiments. This work was performed at the University of Colorado Boulder and Institute of Arctic and Alpine Research. TG and JTML were supported by NASA's Sea Level Change Team (award #80NSSC20K1123) and NSL and CN are grateful for funding from the U.S. Department of Energy (DE-SC0022243). NSL's contributions were additionally funded by the National Science Foundation's Division of Ocean Sciences (#1752724).

References

Aiken, C. M., & England, M. H. (2008). Sensitivity of the present-day climate to freshwater forcing associated with Antarctic sea ice loss. *Journal of Climate*, *21*(15), 3936–3946. https://doi.org/10.1175/2007JCLI1901.1

Bintanja, R., Oldenborgh, G. J. V., Drijfhout, S. S., Wouters, B., & Katsman, C. A. (2013). Important role for ocean warming and increased ice-shelf melt in Antarctic sea-ice expansion. *Nature Geoscience*, *6*(5), 376–379. https://doi.org/10.1038/NGEO1767

Bintanja, R., Oldenborgh, G. J. V., & Katsman, C. A. (2015). The effect of increased fresh water from Antarctic ice shelves on future trends in Antarctic sea ice. *Annals of Glaciology*, *56*(69), 120–126. https://doi.org/10.3189/2015AOG69A001

Bronselaer, B., Winton, M., Griffies, S. M., Hurlin, W. J., Rodgers, K. B., Sergienko, O. V., et al. (2018). Change in future climate due to Antarctic meltwater. *Nature*, *564*(7734), 53–58. https://doi.org/10.1038/s41586-018-0712-z

Cabré, A., & Gnanadesikan, A. (2017). Global atmospheric teleconnections and multidecadal climate oscillations driven by southern ocean convection. https://doi.org/10.1175/JCLI-D-16-0741.s1

Curry, J. A., Schramm, J. L., & Ebert, E. E. (1995). Sea ice-albedo climate feedback mechanism. *Journal of Climate*, *8*(2), 240–247. https://doi.org/10.1175/1520-0442(1995)008<0240:SIACFM>2.0.CO;2

Danabasoglu, G., Lamarque, J. F., Bacmeister, J., Bailey, D. A., DuVivier, A. K., Edwards, J., et al. (2020). The community Earth system model version 2 (CESM2). *Journal of Advances in Modeling Earth Systems*, *12*, e2019MS001916. https://doi.org/10.1029/2019MS001916

DeConto, R. M., & Pollard, D. (2016). Contribution of Antarctica to past and future sea-level rise. *Nature*, *531*(7596), 591–597. https://doi.org/10.1038/nature17145

DeConto, R. M., Pollard, D., Alley, R. B., Velicogna, I., Gasson, E., Gomez, N., et al. (2021). The Paris climate agreement and future sea-level rise from Antarctica. *Nature*, *593*(7857), 83–89. https://doi.org/10.1038/s41586-021-03427-0

Depoorter, M. A., Bamber, J. L., Griggs, J. A., Lenaerts, J. T., Ligtenberg, S. R., Broeke, M. R. V. D., & Moholdt, G. (2013). Calving fluxes and basal melt rates of Antarctic ice shelves. *Nature*, *502*(7469), 89–92. https://doi.org/10.1038/nature12567

Fasullo, J. T., & Nerem, R. S. (2018). Altimeter-era emergence of the patterns of forced sea-level rise in climate models and implications for the future. *Proceedings of the National Academy of Sciences of the United States of America*, *115*(51), 12944–12949. https://doi.org/10.1073/pnas.1813233115

Frölicher, T. L., Sarmiento, J. L., Paynter, D. J., Dunne, J. P., Krasting, J. P., & Winton, M. (2015). Dominance of the southern ocean in anthropogenic carbon and heat uptake in CMIP5 models. *Journal of Climate*, *28*(2), 862–886. https://doi.org/10.1175/JCLI-D-14-00117.1

Gilbert, E., & Kittel, C. (2021). Surface melt and runoff on Antarctic ice shelves at 1.5°C, 2°C, and 4°C of future warming. *Geophysical Research Letters*, *48*(8), e2020GL091733. https://doi.org/10.1029/2020GL091733

Gorte, T., Lovenduski, N., Nissen, C., & Lenaerts, J. T. (2023a). CESM2 CONTROL simulation output: Antarctic ice sheet freshwater discharge drives substantial southern ocean changes over the 21st century [Dataset]. Zenodo. https://doi.org/10.5281/zenodo.8056558

Gorte, T., Lovenduski, N., Nissen, C., & Lenaerts, J. T. (2023b). CESM2 IMBIE simulation output: Antarctic Ice Sheet freshwater discharge drives substantial southern ocean changes over the 21st century [Dataset]. Zenodo. https://doi.org/10.5281/zenodo.8058223

Heuzé, C. (2021). Antarctic bottom water and north Atlantic deep water in CMIP6 models. *Ocean Science*, *17*(1), 59–90. https://doi.org/10.5194/os-17-59-2021

Heuzé, C., Heywood, K. J., Stevens, D. P., & Ridley, J. K. (2013). Southern ocean bottom water characteristics in CMIP5 models. *Geophysical Research Letters*, *40*(7), 1409–1414. https://doi.org/10.1002/grl.50287

Jacobs, S. S., & Giulivi, C. F. (2010). Large multidecadal salinity trends near the Pacific-Antarctic continental margin. *Journal of Climate*, *23*(17), 4508–4524. https://doi.org/10.1175/2010JCLI3284.1

Landerer, F. W., & Swenson, S. C. (2012). Accuracy of scaled grace terrestrial water storage estimates. *Water Resources Research*, *48*(4). https://doi.org/10.1029/2011WR011453

Lenaerts, J. T. M., Bars, D. L., van Kampenhout, L., Vizcaino, M., Enderlin, E. M., & van den Broeke, M. R. (2015). Representing Greenland ice sheet freshwater fluxes in climate models. *Geophysical Research Letters*, *42*(15), 6373–6381. https://doi.org/10.1002/2015GL064738

Li, Q., Marshall, J., Rye, C. D., Romanou, A., Rind, D., & Kelley, M. (2023). Global climate impacts of Greenland and Antarctic meltwater: A comparative study. *Journal of Climate*, *36*(11), 3571–3590. https://doi.org/10.1175/JCLI-D-22-0433.1

Lockwood, J. W., Dufour, C. O., Griffies, S. M., & Winton, M. (2021). On the role of the Antarctic slope front on the occurrence of the Weddell sea polynya under climate change. *Journal of Climate*, *34*(7), 2529–2548. https://doi.org/10.1175/JCLI-D-20-0069.1

Menviel, L., Spence, P., & England, M. H. (2015). Contribution of enhanced Antarctic bottom water formation to Antarctic warm events and millennial-scale atmospheric CO_2 increase. *Earth and Planetary Science Letters*, *413*, 37–50. https://doi.org/10.1016/j.epsl.2014.12.050

Moorman, R., Morrison, A. K., & Hogg, A. M. C. (2020). Thermal responses to Antarctic ice shelf melt in an eddy-rich global ocean-sea ice model. *Journal of Climate*, *33*(15), 6599–6620. https://doi.org/10.1175/JCLI-D-19-0846.1

Nissen, C., Timmermann, R., Hoppema, M., Gürses, Ö., & Hauck, J. (2022). Abruptly attenuated carbon sequestration with Weddell sea dense waters by 2100. *Nature Communications*, *13*(1), 3402. https://doi.org/10.1038/s41467-022-30671-3

Noble, T. L., Rohling, E. J., Aitken, A. R., Bostock, H. C., Chase, Z., Gomez, N., et al. (2020). The sensitivity of the Antarctic ice sheet to a changing climate: Past, present, and future. *Reviews of Geophysics*, *58*(4), e2019RG000663. https://doi.org/10.1029/2019RG000663

Park, W., & Latif, M. (2019). Ensemble global warming simulations with idealized Antarctic meltwater input. *Climate Dynamics*, *52*(5–6), 3223–3239. https://doi.org/10.1007/s00382-018-4319-8

Pattyn, F., & Morlighem, M. (2020). The uncertain future of the Antarctic ice sheet. *Science*, *367*(6484), 1331–1335. https://doi.org/10.1126/science.aaz5487

Pauling, A. G., Bitz, C. M., Smith, I. J., & Langhorne, P. J. (2016). The response of the southern ocean and Antarctic sea ice to freshwater from ice shelves in an Earth system model. *Journal of Climate*, *29*(5), 1655–1672. https://doi.org/10.1175/JCLI-D-15-0501.1

Purich, A., & England, M. H. (2023). Projected impacts of Antarctic meltwater anomalies over the twenty-first century. *Journal of Climate*, *36*(8), 2703–2719. https://doi.org/10.1175/jcli-d-22-0457.1

Rignot, E., Mouginot, J., Scheuchl, B., van den Broeke, M., van Wessem, M. J., & Morlighem, M. (2019). Four decades of Antarctic ice sheet mass balance from 1979–2017. *Proceedings of the National Academy of Sciences of the United States of America*, *116*(4), 1095–1103. https://doi.org/10.1073/pnas.1812883116

Sadai, S., Condron, A., DeConto, R., & Pollard, D. (2020). Future climate response to Antarctic ice sheet melt caused by anthropogenic warming. *Science Advances*, *6*(39), eaaz1169. https://doi.org/10.1126/sciadv.aaz1169

Schwalm, C. R., Glendon, S., Duffy, P. B., & Dickinson, R. E. (2020). Rcp8.5 tracks cumulative CO_2 emissions. *Proceedings of the National Academy of Sciences of the United States of America*, *117*(33), 19656–19657. https://doi.org/10.1073/pnas.2007117117

Shepherd, A., Ivins, E., Rignot, E., Smith, B., Broeke, M. V. D., Velicogna, I., et al. (2018). In *Mass balance of the Antarctic ice sheet from 1992 to 2017* (Vol. 558). Nature Publishing Group. https://doi.org/10.1038/s41586-018-0179-y

Swart, N. C., & Fyfe, J. C. (2013). The influence of recent Antarctic ice sheet retreat on simulated sea ice area trends. *Geophysical Research Letters*, *40*(16), 4328–4332. https://doi.org/10.1002/GRL.50820

Trusel, L. D., Frey, K. E., Das, S. B., Karnauskas, K. B., Munneke, P. K., Meijgaard, E. V., & Broeke, M. R. V. D. (2015). Divergent trajectories of Antarctic surface melt under two twenty-first-century climate scenarios. Retrieved from www.nature.com/naturegeoscience

Velicogna, I., & Wahr, J. (2006). Measurements of time-variable gravity show mass loss in Antarctica. *Science*, *311*(5768), 1754–1756. https://doi.org/10.1126/science.1123785

References From the Supporting Information

Hansen, J., Sato, M., Hearty, P., Ruedy, R., Kelley, M., Masson-Delmotte, V., et al. (2016). Ice melt, sea level rise and superstorms: Evidence from paleoclimate data, climate modeling, and modern observations that 2C global warming could be dangerous. *Atmospheric Chemistry and Physics*, *16*(6), 3761–3812. https://doi.org/10.5194/acp-16-3761-2016

Swart, N., Martin, T., Beadling, R., Chen, J.-J., England, M. H., Farneti, R., et al. (2023). *The southern ocean freshwater release model experiments initiative (SOFIA): Scientific objectives and experimental design* (pp. 1–30). EGUsphere. https://doi.org/10.5194/egusphere-2023-198

Erratum

In the originally published version of this article, the surname of the third author, Cara Nissen, was incorrectly published as "Nisssen." This error appeared in the main author list, the citation, and in Supporting Information S1. The error has been corrected, and this may be considered the authoritative version of record.